Journal of Hydrology 679 (2026) 136163

Contents lists available at ScienceDirect

Journal of Hydrology

journal homepage: www.elsevier.com/locate/jhydrol

Research papers

# Diverging hydrometeorological drivers of flashier floods in a warming climate

Fengjia Zhou [a], Shuo Wang [a,b,*], Louise Slater [c], Peirong Lin [d], Hanbo Yang [e], Sijie Tang [a,f], Amir AghaKouchak [g,h,i]

[a] State Key Laboratory of Climate Resilience for Coastal Cities, Department of Land Surveying and Geo-Informatics, The Hong Kong Polytechnic University, Hong Kong, China
[b] Otto Poon Research Institute for Climate-Resilient Infrastructure and Research Institute for Land and Space, The Hong Kong Polytechnic University, Hong Kong, China
[c] School of Geography and the Environment, University of Oxford, Oxford, UK
[d] Institute of Remote Sensing and GIS, School of Earth and Space Sciences, Peking University, Beijing, China
[e] State Key Laboratory of Hydroscience and Engineering, Department of Hydraulic Engineering, Tsinghua University, Beijing 100084, China
[f] School of Environmental Science and Engineering, Southern University of Science and Technology, Shenzhen, China
[g] Department of Civil and Environmental Engineering, University of California, Irvine, Irvine, CA, USA
[h] Department of Earth System Science, University of California, Irvine, CA, USA
[i] United Nations University Institute for Water, Environment and Health, Richmond Hill, ON, Canada

ARTICLE INFO

This manuscript was handled by Yuefei Huang, Editor-in-Chief, with the assistance of Jing-Cheng Han, Associate Editor

*Keywords:*
Flash flood
Climate change
Explainable machine learning

ABSTRACT

The monitoring and forecasting of flash floods present significant challenges due to their rapid onset. While extreme rainfall events, a primary driver of flooding, are becoming flashier, there is no consensus on whether floods will exhibit similar trends in a warming climate. Here, we assess flash flood risk development over four decades across 741 basins globally using the flashiness index. Our findings reveal a significant shift towards flashier floods in nearly one-third of the basins, predominantly concentrated in cold and arid regions of the northern mid-latitudes. In these regions, the increase in flashiness is largely associated with larger flood peaks rather than changes in timing. We identify basins characterised by rising flood peaks, which are likely to require flood defence infrastructure capable of withstanding more severe flood events, as well as those marked by shorter onset times, which may face challenges in implementing short-term early warning systems. Specifically, the increase in flashiness in most North American basins is mainly associated with rising flood peaks, whereas in most European basins, it is dominated by shorter onset times. These findings underscore the urgency of implementing region-specific strategies to adapt to flashier floods in a warmer future.

## 1. Introduction

Flooding is one of the most widespread and devastating natural disasters (Hirabayashi et al., 2013; Jongman et al., 2014; You et al., 2024; Zhou et al., 2025), exposing over one-fifth of the world's population to significant risk (Rentschler et al., 2022) and causing annual global economic losses of $210 billion (Benfield, 2016). With climate change, the risk of loss of life and welfare due to flooding is projected to increase further in the future (Dottori et al., 2018). Flash floods are a type of flood that occurs within a short period, usually from minutes to several hours (Gourley et al., 2013). They provide limited time for early warning, often leading to devastating impacts. Despite a long history of related research, flash floods have garnered increasing attention due to the significant challenges they pose to flood control infrastructure and governmental mitigation strategies.

Numerous studies quantify flash flood risks and identify contributing factors. A widely adopted approach is to estimate the total rainfall required to produce bankfull flow, a condition that often triggers flash floods, and dynamically assess the impact of rainfall on the basin to predict the probability of flash flood occurrence within a short period. Building on this approach, several studies have identified an increasing trend in both the frequency and intensity of flash floods in certain regions, indicating a growing flash flood risk (Alipour et al., 2020b; Georgakakos et al., 2022; Yin et al., 2023). However, this method does

* Corresponding author at: State Key Laboratory of Climate Resilience for Coastal Cities, Department of Land Surveying and Geo-Informatics, The Hong Kong Polytechnic University, Hong Kong, China.
*E-mail address:* shuo.s.wang@polyu.edu.hk (S. Wang).

https://doi.org/10.1016/j.jhydrol.2026.136163
Received 17 March 2026; Received in revised form 31 May 2026; Accepted 1 August 2026
Available online 3 August 2026

not account for the full continuum of land surface responses to extreme rainfall and river routing processes. A river flow-based method can address this issue, with one key approach being the computation of indices that characterise the rapidity of floods and exploring their response to potential drivers (Bhaskar et al., 2000). The Richards-Baker Flashiness Index, originally proposed in 2004, reflects the frequency and rapidity of short-term changes in daily streamflow (Baker et al., 2004). Subsequently, the concept of flashiness was refined to the hourly time-scale, and other variants were developed to quantify the severity, frequency, and duration of flood events (Li et al., 2023; Saharia et al., 2017). Using these indices, studies have reported a trend towards flashier floods in the United States, driven by climate change (Li et al., 2022).

Although global extreme rainfall, a key driver of floods, has shown a tendency towards shorter durations with more pronounced peaks (Donat et al., 2016; Fowler et al., 2021; Guerreiro et al., 2018; Ragno et al., 2018; Wasko et al., 2021), no consensus has been reached on whether there has been a transition to flashier floods at the global scale. Time to peak and peak magnitude, the two most directly related characteristics to the rising limb of a flood hydrograph, are considered alongside the rising limb as the three key features of flash floods (Bhaskar et al., 2000). Previous studies, however, have typically treated flash floods uniformly, failing to distinguish between different drivers that influence the distinct characteristics of flashier floods under climate change (Chen et al., 2022; Li et al., 2023; Saharia et al., 2017; Zhong et al., 2020). In this study, we used the Global Reach-Level Flood Reanalysis (GRFR) dataset (Yang et al., 2021) and applied an event-based flashiness index to investigate changes in the speed of global flood onset. We propose a new classification method that categorises flashier floods into two types: those dominated by larger flood peaks (hereafter referred to as Q-dominated) and those dominated by shorter onset times (hereafter referred to as T-dominated). Using advanced explainable machine learning, we quantify the impact of meteorological drivers on changes in flood flashiness across different regions worldwide. For each classification of flashier floods, we conduct distinct attribution analyses using explainable machine learning, providing insights into flood hazards and prevention strategies under various changing scenarios. This study aims to provide a comprehensive, in-depth assessment of changes in global flood flashiness. The results could serve as a basis for adapting global flood planning strategies and advocating climate-resilient mitigation measures for emerging flash flood hotspots.

## 2. Methodology

### 2.1. Definition of event-based, river reach-based and basin-based flashiness

The definition of “flashiness” can be categorised into three types: event-based, river reach-based and basin-based. Event-based flashiness usually refers to the difference between the peak discharge and the action stage discharge, normalised by the time to peak (Fig. 1). Based on flood events from the GRFR dataset (https://www.reachhydro.org/home/records/grfr) (Yang et al., 2021), the action stage is defined as the first record of each flood event, and the peak discharge is the maximum flow rate during a flood event. Floods in basins of varying sizes exhibit significant differences in both magnitude and temporal development. To ensure that event-based flashiness remains comparable across different basins, the rising limb slope is standardised by the basin area, as given in Eq. (1) (Li et al., 2022).

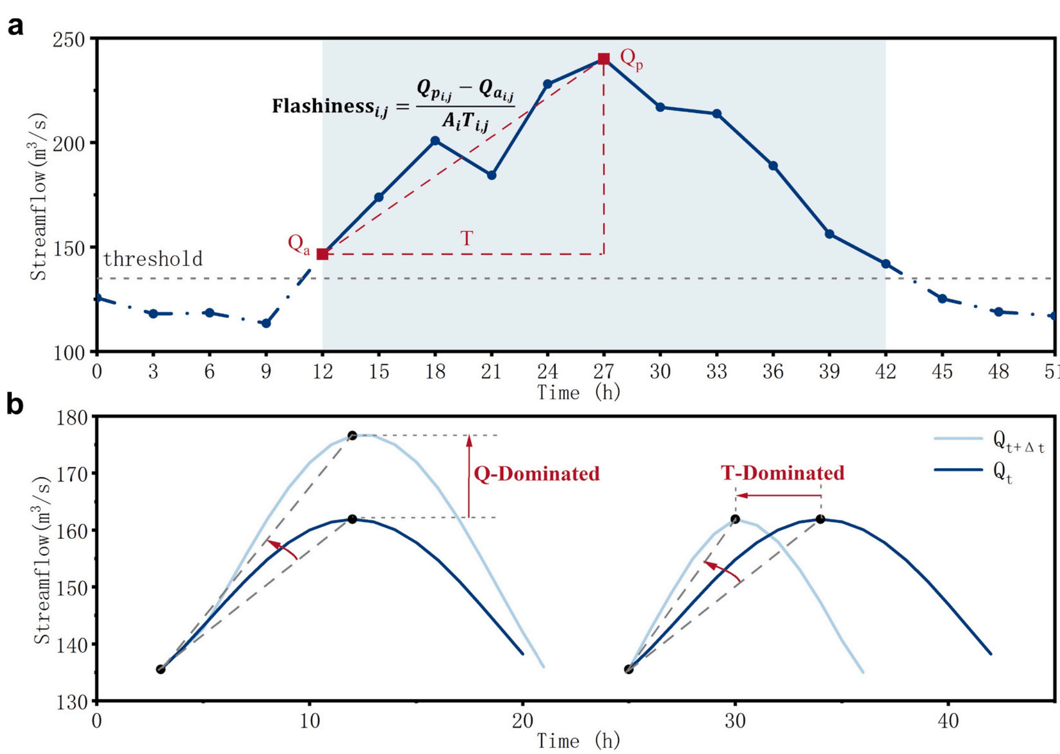


**Fig. 1.** Definition of flashiness and classification of increasing flashiness. (a) Schematic representation of event-level flashiness. The solid blue line represents flood discharge above the 2-year return period threshold (dashed grey line), while the dash-dotted blue line indicates discharges below the threshold, which are set to zero in the GRFR data. The blue shaded area represents the flood event period, with the flood peak being the maximum flow during this period (Qp). The action stage is the first recorded flow during the flood period (Qa). Flashiness is calculated as the slope between Qa and Qp, divided by the catchment area. (b) Schematic representation of two categories of increasing flashiness. The dark blue line represents flood events occurring before the increase in flashiness, while the light blue line represents flood events after the increase in flashiness. (For interpretation of the references to colour in this figure legend, the reader is referred to the web version of this article.)

$$Flashiness_{i,j} = \frac{Q_{p_{i,j}} - Q_{a_{i,j}}}{A_i T_{i,j}} \tag{1}$$

where $Q_p$ and $Q_a$ refer to the peak discharge and the action stage discharge of a flood event, respectively (Fig. 1). The indices $i$ and $j$ indicate each river reach and flood event, respectively. $A$ and $T$ represent the catchment area and time to peak, respectively. This normalisation expresses the discharge increase from action stage to flood peak as an area-specific rate of flood intensification, reducing the direct influence of basin size on absolute discharge changes. However, catchment area does not capture all hydrogeomorphic controls on flashiness; other factors, such as reach length, slope, upstream drainage area, and unit catchment area, are considered separately in the attribution analysis.

Basin-based flashiness refers to the risk of flash flooding in a specific basin, which is aggregated from river reach-based flashiness. An empirical cumulative distribution function (ECDF) is used to scale the event-based flashiness values between 0 and 1. The standardised version of flashiness is

$$\widetilde{F_{i,j}} = \frac{1}{\sum_{i=1}^{S} N_i} \sum_{i=1}^{S} \sum_{j=1}^{N_i} I_{(\text{Flashiness} \leq t)} \tag{2}$$

where $\widetilde{F_{i,j}}$ represents the flashiness value normalised using the empirical cumulative distribution function. $I_{(\text{Eq})}$ is the indicator function yielding 1 if the condition Eq is true and 0 otherwise.

Event-level flashiness given in Eq. (2) is computed for all flooding events. Following Li et al. (2022), the characteristic scaled flashiness variable for a given river reach or basin $i$ is summarised by the median value computed from all flooding events $N_i$ observed at that area. The median provides a robust estimate of typical event-based flashiness and reduces the influence of a few exceptionally extreme events.

$$\left[\widetilde{F}_i : P\left(\widetilde{F_{i,j}} \leq \widetilde{F}_i\right)\right] = \frac{1}{2}, \text{for} j \in \{1, \cdots, N_i\} \tag{3}$$

where $P$ represents the probability that the random variable $\widetilde{F_{i,j}}$ takes on a value less than or equal to $\widetilde{\mathrm{F}}_{\mathrm{i}}$.

The difference in river reach-based flashiness between 1980–1999 and 2000–2019 represents the change in flashiness for each river reach. This approach is adopted due to the insufficient number of events to conduct a trend analysis. Specifically, certain years may lack flood events entirely, while others may experience multiple occurrences. Such gaps can impact trend analyses, and variations in the frequency and magnitude of flood events can introduce significant uncertainty. The significance of these changes was tested using the Mann-Whitney $U$ test and the Kolmogorov-Smirnov test. To account for multiple comparisons across the large number of Level 4 basins, we applied the Benjamini–Hochberg false discovery rate (FDR) (Benjamini & Hochberg, 1995) correction separately to the p-values from each test. Basins were classified as experiencing a significant increase in flashiness only when the percent change was positive and both FDR-adjusted p-values were below 0.05.

### 2.2. *Classification of flood flashiness*

Since flashiness encompasses both flood magnitude and temporal development, the increase in flood flashiness is categorised into two types (Fig. 1b): (a) Flashier floods dominated by larger flood peaks (Q-dominated): the increase in flood flashiness is primarily attributed to the rise in peak flow rates, while the onset time of floods has not shown a significant trend or is lengthening (which typically results in reduced flashiness). (b) Flashier floods dominated by shorter onset times (T-dominated): the increase in flood flashiness is primarily attributed to the shortening of onset time, while the peak flow rates have not shown a significant trend or have decreased. This classification was applied only to basins that exhibited a significant increase in flashiness. For each of these basins, we separately evaluated the temporal trends in flood peak discharge and onset time for all river reaches using the Mann–Kendall test (see Fig. S1 in Supporting Information S1). Only statistically significant reach-level trends were considered in the classification, while non-significant trends were excluded. A basin was classified as Q-dominated if more than half of its river reaches with significant flood-peak trends showed increasing peak discharge, and as T-dominated if more than half of its river reaches with significant onset-time trends showed decreasing onset time. If both criteria were met, the basin was classified as a Q-T compound basin, indicating the coexistence of increasing flood peaks and shortening onset times.

### 2.3. *Attribution of flood flashiness using explainable machine learning*

We used the machine learning model LightGBM (Ke et al., 2017), with the training and testing targets being the event-based flashiness of each river reach. Model inputs comprised static features of the river reaches and dynamic features of flood events. Static features included length, slope, upstream drainage basin area, and unit catchment area, which were derived from underlying hydrography data in the GRFR. Dynamic features included upstream flooding and meteorological variables at the time of flood occurrence. To quantify the transfer of floodwaters from upstream to downstream reaches, we identified the peak discharge in the upstream river reaches during the 24-hour period preceding the onset of flooding in the local reach, using this as an indicator of flood transfer from the upstream basin. Meteorological inputs consisted of daily average temperature, soil moisture, snowmelt and cumulative rainfall on the day of flood onset. The river reaches at a resolution of 0.05° were spatially matched to gridded meteorological data, with the grid value, or the average of multiple grids, used as the corresponding meteorological driver for each river reach. We optimised the LightGBM model structure hyperparameters using grid search combined with 5-fold random cross-validation. The optimisation space of the parameters and the optimal hyperparameter combinations are shown in Table S1 in Supporting Information S1.

The SHapley Additive exPlanations (SHAP) approach is a game theory-based method for calculating the impact of each feature on the prediction target (Shapley, 1953). It addresses the challenge of interpreting machine learning results. The SHAP value represents the contribution of each feature to each individual prediction (Lundberg and Lee, 2017). A SHAP value greater than zero indicates a positive contribution from a feature to the mean prediction of the response variable (here, flashiness), and vice versa. Feature importance is defined as the absolute sum of all positive and negative contributions from each feature. SHAP values were computed using the Python scikit-learn library (Pedregosa et al., 2011), the "shap" package (https://github.com/slundberg/shap), and the TreeSHAP function (Lundberg et al., 2020).

## 3. Data

### 3.1. *Flood data*

3-hourly river flood data were obtained from Global Reach-Level Flood Reanalysis (GRFR) (https://www.reachhydro.org/home/records/grfr) (Yang et al., 2021). The use of modelled data is driven by the fact that only a small portion of global rivers are represented by gauges, and studies on flash floods require global sub-daily flow data. This dataset is a product of the VIC land surface model (0.05°, 3-hourly) which is well-calibrated and bias-corrected and the RAPID routing model (2.94 million river and catchment vectors), which was originally developed by Lin et al. (2019) as a daily product (GRADES) and updated to 3-hourly products in GRFR. The results have been assessed against 3-hourly flow records from over 6000 gauges in CONUS and daily records from more than 14,000 gauges globally (Yang et al., 2021). Correlation coefficients ranged from 0.5 to 0.9 for daily flows and 0.7 to 0.9 for monthly flows. Approximately 44% of the gauges exhibited a relative bias of less than ±20%. Generally, simulations are more accurate in humid regions than arid regions. In the CONUS region, 74% of gauges achieved correlation coefficients greater than 0.5 when validated with 3-hourly data. To further assess the data's reliability, in this study, we validated 3-hourly model outputs against a screened subset of 4123 sites. Selection criteria required less than 30% missing data and records exceeding 10 years in length. Our validation results align closely with the aforementioned findings (see Fig. S2 in Supporting Information S1). We further validated GRFR against the independent EuroMedeFF flash-flood database, using 218 event-station/reach hydrograph comparisons from 26 documented events. The correlations were generally acceptable, and cases with negative correlations were mainly attributable to timing offsets rather than missed flood responses, as shown by a ±24 h lag sensitivity test (Fig. S3). Additionally, previous studies have acknowledged the data's proven global applicability and its effectiveness in representing hydrological processes across diverse regions (Feng & Gleason, 2024). These findings indicate that the model performs well and accurately reconstructs flood events, including extreme values.

GRFR data include 3-hourly and daily naturalised river discharge, global 3-hourly river flood events from 1980 to 2019, and the underlying hydrography data provided by MERIT-Basins (Lin et al., 2019). In the GRFR flood-event product, flood events are extracted using a 2-year return-period threshold, and discharge values below this threshold are set to zero. To test whether the flashiness metric is sensitive to this threshold, we conducted an additional sensitivity analysis using an approximated 3-year return-period threshold. The resulting river reach-based flashiness is highly consistent with that derived from the original 2-year threshold (Fig. S4), indicating that our flashiness estimates are not strongly dependent on the threshold choice.

### 3.2. Climate data

Hourly soil moisture, temperature, and snowmelt data at a 0.25° spatial resolution for the period 1980–2019 were obtained from the fifth generation of European ReAnalysis (ERA5) dataset (Hersbach et al., 2020) (https://cds.climate.copernicus.eu/). The gridded data were further spatially aggregated to correspond to each river reach and temporally aggregated to daily scale. Daily precipitation data were calculated from MSWEP version 2.2 (Beck et al., 2017) (https://www.gloh2o.org/mswep/). MSWEP is a global precipitation product with a 3-hourly 0.1° resolution available from 1979 to the present. It compares better with Stage IV gauge–radar data than other global precipitation datasets (Beck et al., 2019; Feng & Gleason, 2024). Precipitation was partitioned into rainfall and snowfall on the basis of daily temperature using the following empirical model (Zhu et al., 2022):

$$Rainfall = \begin{cases} P \text{ for } Temp_a \geq Temp_{\mathrm{rain}} \\ P\left(\dfrac{Temp_a - Temp_{\mathrm{snow}}}{Temp_{\mathrm{rain}} - Temp_{\mathrm{snow}}}\right) \text{ for } Temp_{\mathrm{snow}} \leq Temp_a \leq Temp_{\mathrm{rain}} \\ 0 \text{ for } Temp_a < Temp_{\mathrm{snow}} \end{cases} \tag{4}$$

where P is precipitation (mm) and $Temp_a$ is average daily air temperature (°C). Partitioning thresholds $Temp_{\mathrm{rain}}$ and $Temp_{\mathrm{snow}}$ are 3.0 and −1.0 °C, respectively.

These meteorological datasets are consistent with the inputs of the underlying model used in the GRFR dataset, ensuring coherence in the data analysis.

## 4. Results

### 4.1. Spatial distribution of flashiness and its variations

Based on all flood events identified using the GRFR dataset from 1980 to 2019, river reach-based flashiness was examined globally. The flashiness quantifies the overall rapidity of flood occurrences in a river reach, measured by the slope of the rising limb of flood events within the reach, using statistical methods. River reaches with high flashiness are predominantly concentrated in tropical climate zones (Beck et al., 2006), which are also the wettest regions in the world (Konapala et al., 2020), including Central America and the northern part of South America, Central Africa, South Asia, and Southeast Asia (Fig. 2a, c). On average, flash floods account for 61% of all flood events in these regions. As the occurrence of floods is commonly generated by rainfall, soil moisture, and snowmelt (Zhang et al., 2022), we examined the statistical relationships between flashiness and these underlying meteorological drivers (Fig. 3). We found that flood events with high flashiness frequently occur under conditions of high rainfall and high temperature levels. This may be due to the fact that heat waves are often followed by heavy rainfall, a phenomenon potentially linked to atmospheric convection and moisture convergence, which can increase the likelihood of flash floods (You & Wang, 2021). For soil moisture, while a small subset of floods (<5%) with higher flashiness occurs under extremely dry conditions (SM < 0.1 $m^3m^{-3}$), the flashiness of most flood events increases with rising soil moisture levels (Fig. 3b). Across all river basins worldwide, river reaches with high flashiness and those with low flashiness are interspersed. This pattern arises because flashiness is influenced not only by climatic conditions but also by topographic factors. For example, previous studies have identified that flashiness exhibits positive correlations with channel slope and catchment slope, and a negative correlation with drainage area (Li et al., 2023; Saharia et al., 2017).

We aggregated changes in river reach flashiness to Level 4 basins as defined by the HydroBASINS dataset for global analysis (Lehner & Grill, 2013). The HydroBASINS product utilises the 'Pfafstetter' coding system, which provides a global hierarchical breakdown of basins into 12 sub-basin levels. Level 4 basins strike an optimal balance, capturing spatial heterogeneity within individual basins while maintaining the broader spatial patterns necessary for global analysis. Larger basins may fail to account for internal spatial variability, while smaller basins might obscure broader global trends. Based on the FDR-corrected significance tests, nearly one-third of the basins experienced a significant increase in flood flashiness from 1980–1999 to 2000–2019. This increase is predominantly observed in North America, the northwestern part of Asia, Europe, and the eastern part of Africa and South America (Fig. 2b). Latitudinally, significant increases in flashiness are more frequently observed in the mid-latitudes of the Northern Hemisphere (Fig. 4a). Notably, basins with inherently high river reach-based flashiness, such as those in Southeast Asia, South Asia, and Central Africa, have either not exhibited significant changes or have shown significant decreases in flashiness. The regions experiencing more substantial changes in flashiness are concentrated in basins with relatively moderate flashiness (Fig. 4b). In other words, the majority of basins with lower flash flood risk are experiencing a shift to flashier floods in recent decades. To test whether these spatial patterns are sensitive to methodological choices, we conducted two robustness checks. First, we repeated the analysis using the mean ECDF instead of the median ECDF to derive basin-based flashiness. The resulting spatial patterns and directions of change remain generally consistent (Fig. 5). Second, we tested the sensitivity of flashiness changes to alternative temporal windows, including 1980–1994 versus 2005–2019 and 1980–2000 versus 2001–2019. These alternative comparisons reproduced the main spatial patterns of flashiness change, indicating that the identified hotspots are broadly robust to the choice of temporal window (see Fig. S5 in Supporting Information S1).

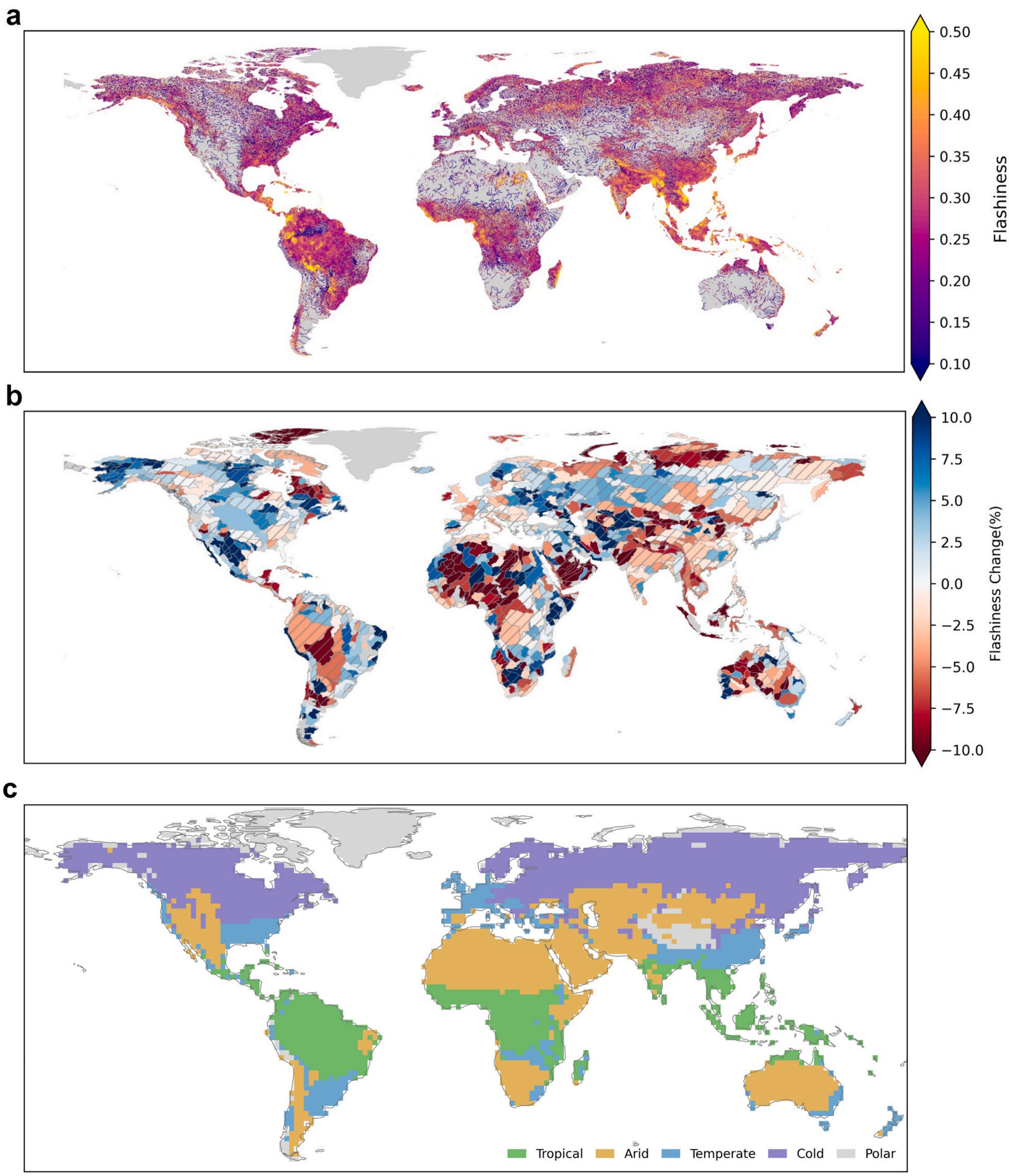


**Fig. 2.** Global patterns of river reach-based flashiness, its temporal changes, and climatic context. (a) Present-day flashiness indices calculated for the period 1980 to 2019. (b) Percent change from the early period (1980–1999) to the later period (2000–2019) in the flashiness indices at the Level 4 basin. Basins marked with grey diagonal stripes indicate a significant increase in flashiness between the two periods, defined as a positive percent change with both Mann–Whitney U and Kolmogorov–Smirnov tests remaining significant after Benjamini–Hochberg FDR correction at the 5% level. (c) Major Köppen–Geiger climate zones, grouped into tropical, arid, temperate, cold, and polar classes.

Given that basins with significant increases in flashiness tend to experience greater negative human impacts than those with decreases, this study focuses on these significantly flashier basins. We categorise flashier basins into two types based on the characteristics of the floods. According to our classification, the majority of basins exhibiting transitions towards flashier flooding are Q-dominated (see Fig. S6 in Supporting Information S1), indicating that these basins have experienced increased flood intensity over comparable time scales. These basins are concentrated in northern North America, western Siberia, and western and southern Africa. T-dominated basins are relatively few; about half the area of Q-dominated ones, and are mainly concentrated at the Asian-European interface. The primary shift in these basins towards flash floods is characterised by a faster timing of flood events on a subdaily scale. Generally, Q-dominated or T-dominated basins suggest that the increase in flood flashiness manifests either as larger flood magnitudes or as more rapid peak attainment. Regardless of the form,

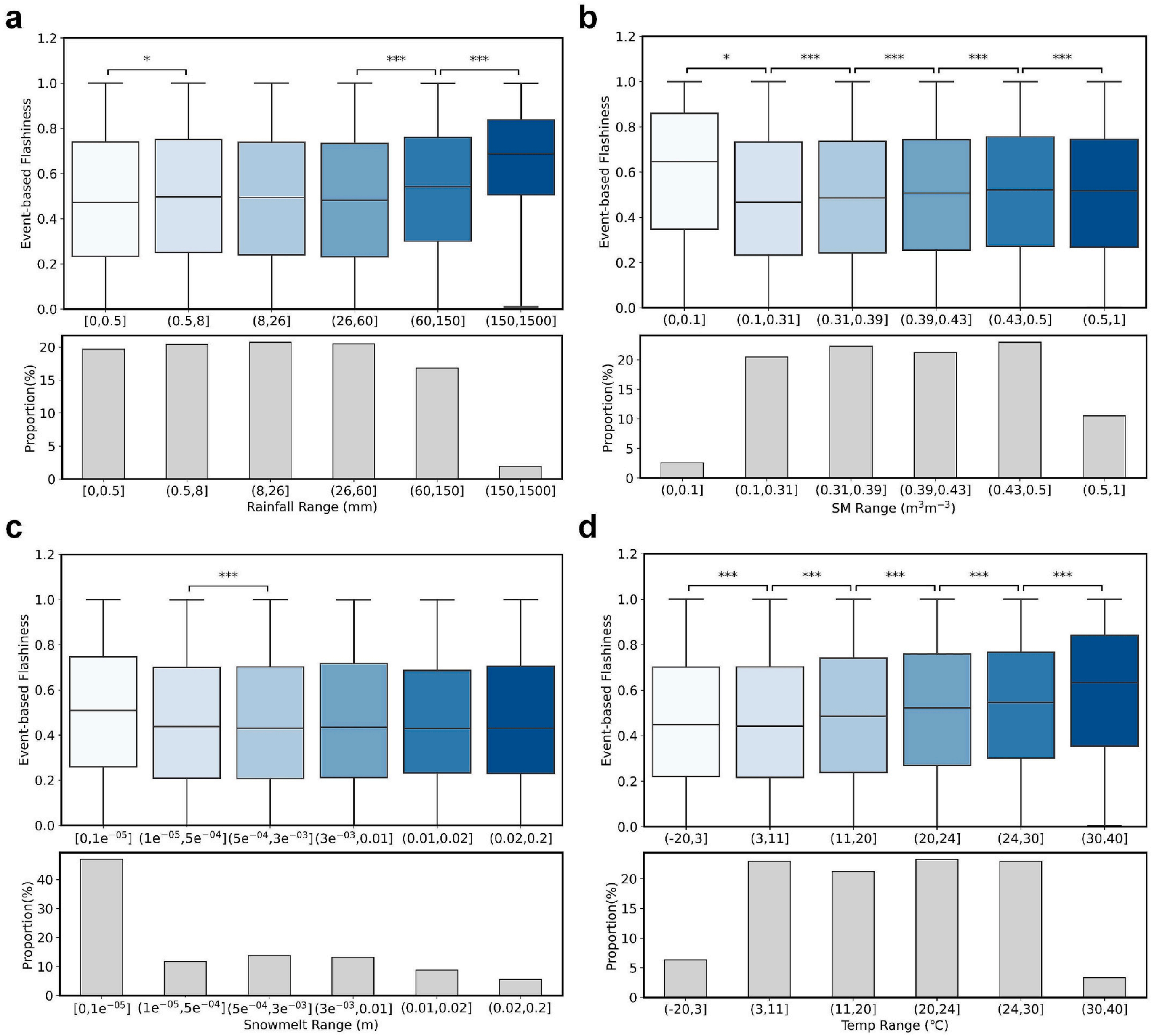


**Fig. 3.** Relationship between event-based flashiness and different factors. The upper panels (a–d) display boxplots of flashiness statistics across varying ranges of key factors: (a) rainfall, (b) soil moisture, (c) snowmelt, (d) temperature. Whiskers represent the 1st and 99th percentiles, the top and bottom of the box are the 25th and 75th percentiles and the median is represented by the horizontal line internal to the coloured box. The lower panels illustrate the percentage of events in each bin. Asterisks (*) indicate statistically significant differences between adjacent bins, with * denoting $p < 0.05$, ** denoting $p < 0.01$ and *** denoting $p < 0.001$.

the rate of flood discharge per unit time has increased, thereby elevating the potential risks posed to affected communities. Additionally, larger flood peaks and shorter onset times may coexist in a basin, which we refer to as a Q-T compound basin, accounting for 25% of all significant flashier basins (see Fig. S6 in Supporting Information S1). All three basin types are predominantly located in cold and arid climatic zones, which collectively account for approximately 75% of all significant flashier basins. In these regions, most of the increase in flashiness is associated with larger flood peaks. While this climate-zone pattern may also reflect the influence of basin morphology and human modification (Gannon et al., 2022; Saharia et al., 2017), the overrepresentation of significantly flashier basins in cold and arid zones suggests that these regions require particular attention to flash flood risks, especially those linked to rising flood peaks.

### 4.2. *Attribution of T-dominated and Q-dominated regions under climate change*

North America and Europe, two regions known for significant economic losses from flooding (Ward et al., 2013), also exhibit high concentrations of significant flashier basins (Fig. 2b, Fig. S7 in Supporting Information S1). On average, these basins have seen a 6.9% rise in flashiness. Past studies have highlighted the severe damage caused by flash floods in these regions. For instance, Barredo (2007) found that 40% of flood-related casualties in Europe between 1950 and 2006 were due to flash floods. On average, Europe records 50 flash flood-related fatalities each year (Sene, 2012). In the United States, over 28,000 flash flood events were reported between 2007 and 2015 (Gourley et al., 2017), and flash floods caused the highest number of casualties among all flood types (Terti et al., 2017). Furthermore, the flash flood hazard in certain areas within Europe and North America, such as the southeast

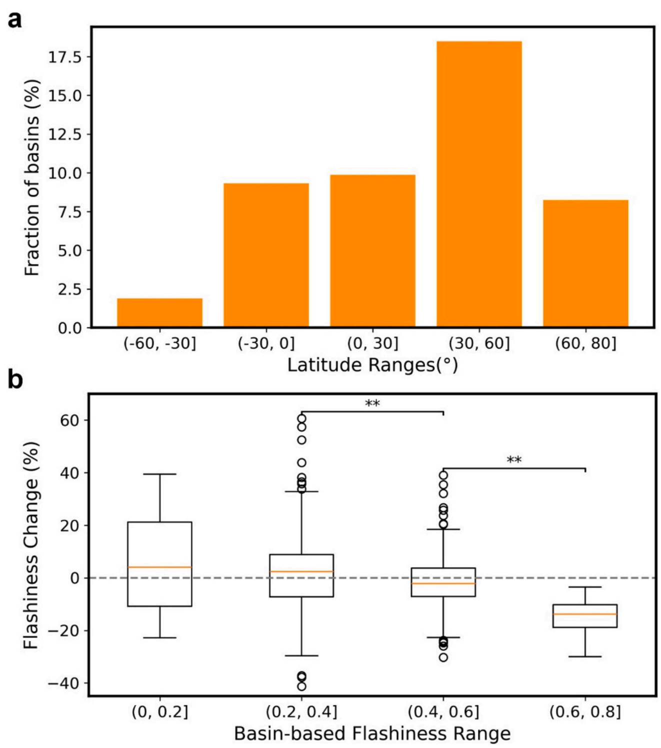


**Fig. 4.** Statistical distribution of flashiness changes in global basins. (a) Statistics on the fraction of global basins experiencing significant flashiness increases at different latitudinal ranges. (b) Percentage change in basins with different flashiness levels from 1980–1999 to 2000–2019. The correlation between basin-based flashiness and flashiness change is −0.2 ($p < 0.001$). Whiskers represent the 1st and 99th percentiles, the top and bottom of the box are the 25th and 75th percentiles and the median is represented by the horizontal line internal to the coloured box. Asterisks (*) indicate statistically significant differences between adjacent bins, with * denoting $p < 0.05$ and ** denoting $p < 0.01$.

United States and central western Europe, as well as central to southern Europe, is expected to rise in both frequency and severity (Alipour et al., 2020b; Marchi et al., 2010; Meyer et al., 2021), with more severe impacts anticipated in these regions (Ahmadalipour & Moradkhani, 2019; Kvočka et al., 2016). A recent example of this trend occurred in late October 2024, when a devastating flash flood in Spain resulted in 224 deaths and 13 missing persons, making it the deadliest disaster in Spain in recent decades (Suardy, 2024).

We observe that flood flashiness is undergoing significant changes in both North America and Europe (see Fig. S8 in Supporting Information S1). Additionally, we identified key flashier basins for further detailed analysis and classified them into Q-dominated and T-dominated categories (Fig. 6). Although Q-T compound basins are the most dangerous category, they account for only 17.5% of all basin types within North America and Europe, and they have the most complex mechanisms. For example, simultaneous increases in flood peaks and reductions in flood response time may be associated with intensified short-duration rainfall, changes in rainfall–runoff efficiency, basin morphology, and human modifications. In addition to hydrometeorological extremes such as heavy rainfall (Fadhel et al., 2018), increased impervious cover and storm drainage have also been reported as factors that can increase peak discharge while reducing catchment response time (Miller et al., 2014; Suriya & Mudgal, 2012). Therefore, for clarity of attribution, we only focus on T-dominated and Q-dominated watersheds separately in our study. In Europe, the ratio of the area of Q-dominated to T-dominated basins is 2:3, while in North America, the majority of basins are Q-dominated, with a ratio of 3:1. Both Q-dominated and T-dominated basins exhibit distinct spatial distribution patterns. For example, in Europe, T-dominated basins are predominantly found in the eastern and western regions, while Q-dominated basins are mainly located in the central region. In North America, Q-dominated basins are primarily distributed in the northern part, consistent with Slater et al.'s findings on changes in flood magnitudes (Slater et al., 2021). Conversely, T-dominated basins are primarily distributed in the southwestern part (Fig. 6b). Given that Q-dominated and T-dominated flashier floods are triggered by different mechanisms, their spatial distributions also vary. We infer that the significant increases in flashiness dominated by these two distinct factors are influenced by different underlying drivers.

Flooding is a complex physical process that can be triggered by multiple mechanisms, usually associated with rainfall, temperature, snowmelt, soil moisture and some topographic factors (Alipour et al., 2020a; Kemter et al., 2020; Sikorska et al., 2015). Furthermore, changes in land use and land cover, along with other anthropogenic factors, significantly influence flooding, particularly in smaller basins (Blöschl et al., 2020; Goodrich et al., 2020; Jodar-Abellan et al., 2019). Traditionally, hydrologic models have been employed to evaluate the drivers of flash floods (Looper & Vieux, 2012; Miao et al., 2016; Nguyen et al., 2016). However, these models often rely on detailed local-scale data, which are frequently unavailable, limiting their applicability (Hapuarachchi et al., 2011). To understand the factors that determine the flashiness of flood events, here we employed Light Gradient-Boosting Machine (LightGBM) models and used SHapley Additive exPlanations (SHAP) values to estimate the contribution of different factors. To capture a comprehensive range of variables influencing flashiness and ensure accurate attribution, we incorporated both hydrological features (e.g., river reach length, slope, upstream drainage basin area, unit catchment area) and meteorological features (e.g., rainfall, temperature, soil moisture, snowmelt on the day of flood onset) of the basin as inputs for the machine learning model. The LightGBM model demonstrates strong out-of-sample prediction performance, with a high ratio of explained variance ($R^2 = 0.72$) (Fig. 7).

Fig. 8a and b show the meteorological features we considered for the flashiness models. While we integrate hydrological features and flood transfer dynamics from upstream basins to enhance the predictive accuracy of our machine learning model, parameters such as reach length, slope, and drainage basin area remain relatively static in the short term. Consequently, our analysis prioritises the impact of meteorological drivers on flashiness variations, particularly in the context of climate change. The feature importance rankings, as estimated by SHAP values, reveal a consistent pattern across both Q-dominated and T-dominated basins. Rainfall emerges as the most critical meteorological variable, followed by temperature. To explore flashiness evolution characteristics and conduct attribution analysis, we divided the basins with significant changes in flashiness into two groups, Q-dominated and T-dominated, and plotted the time series of anomalies of annual flood characteristics (peak flow and onset time) and meteorological factors from 1980 to 2019 (Fig. 8c, d). It is noticeable that there has been no significant change in peak discharge (Qmax) in T-dominated basins (Fig. 8d), indicating that the increase in flashiness is primarily due to a substantial shortening of the onset time. Conversely, in Q-dominated basins, since changes in onset time do not lead to an increase in flashiness, the increase in flashiness is primarily due to a significant increase in flood peak discharge (Fig. 8c).

In Q-dominated basins, SHAP analysis indicates that rainfall is the most significant meteorological contributor to flashiness (Fig. 8a). Although temperature is the second most important predictor, the distribution of SHAP values across varying temperature ranges reveals limited sensitivity differences (see Fig. S9 in Supporting Information S1), suggesting that temperature alone is unlikely to be the driving factor behind increases in flashiness. Among the meteorological predictors related to water quantity, only the 95th quantile of rainfall showed a significant upward trend. In Fig. S9, we observe a positive association between SHAP values and rainfall. This indicates that higher rainfall has a more significant positive contribution to the flashiness of

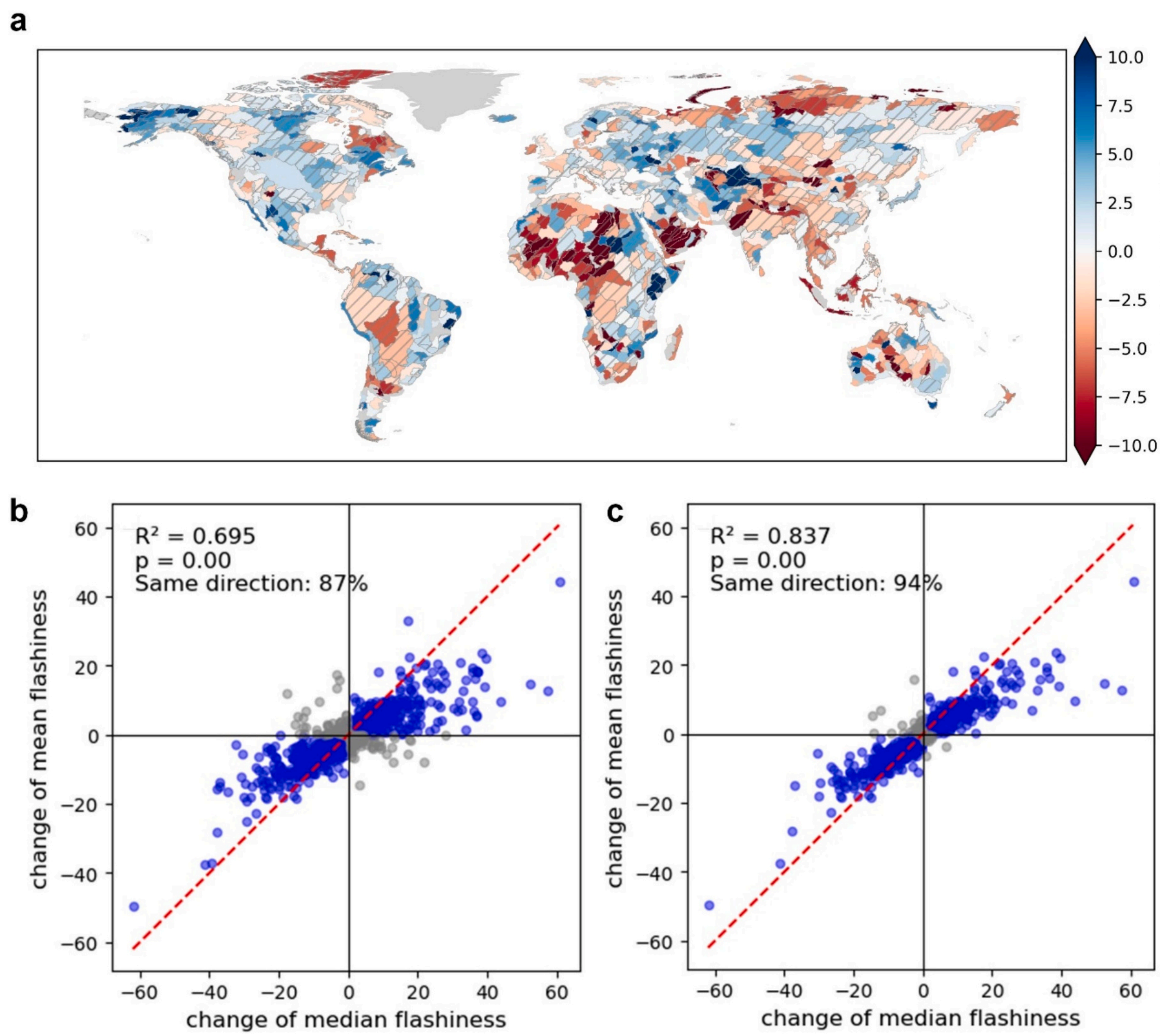


**Fig. 5.** Comparison of flashiness changes aggregated using mean empirical cumulative distribution function (ECDF) versus median ECDF. (a) Similar to Fig. 1b in the main text, but based on mean ECDF. (b and c) validate the direction of flashiness changes calculated using both mean and median ECDF across all basins (b) and significant basins (c).

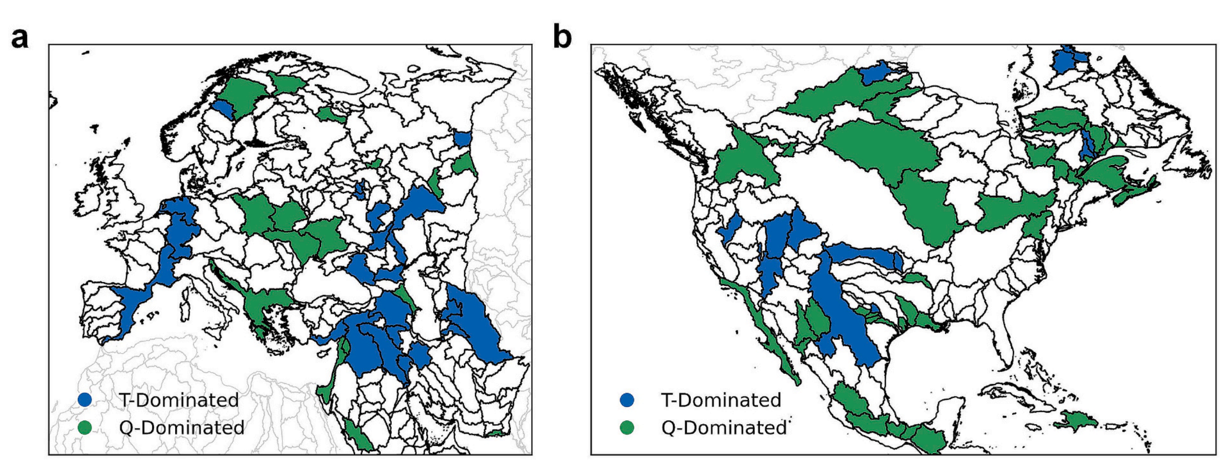


**Fig. 6.** Classification of Level 4 basins with significant increases in flashiness. (a) Classification of basins exhibiting significant increases in flashiness across Europe. The blue regions represent areas in which the increase in flashiness is predominantly influenced by a shortened onset time, whereas the green regions represent areas where the increase in flashiness is primarily influenced by higher flood peak discharge. (b) Similar to a, but for basins across North America. (For interpretation of the references to colour in this figure legend, the reader is referred to the web version of this article.)

floods, with the increase in Qmax being associated with the intensification of extreme rainfall. In addition, the variation of annual

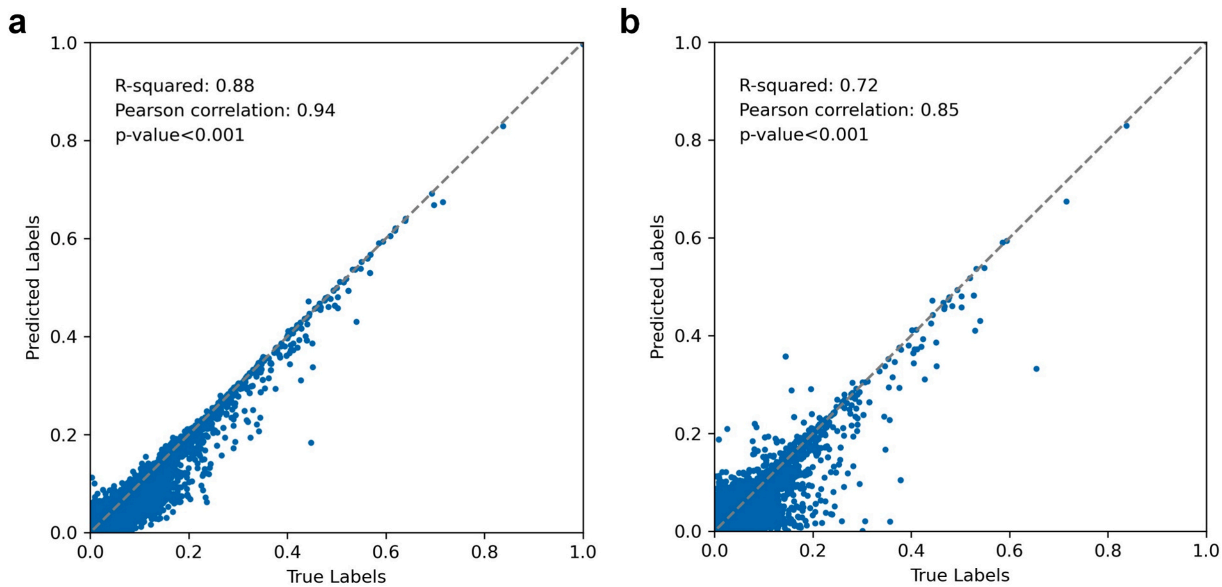


**Fig. 7.** Model performance of LightGBM. (a and b) Scatter density plots of observations and predictions of the LightGBM model for the training (a) and test (b) datasets.

95th-percentile rainfall is similar to the variation in the relative change in annual maximum discharge. Specifically, the relative change in annual maximum discharge increases (decreases) when annual 95th percentile rainfall increases (decreases), suggesting a close association between increasing extreme rainfall and larger flood peaks (Fig. 8c). Thus, the increase in extreme rainfall appears to be the most important meteorological factor associated with increasing flashiness in Q-dominated basins.

In contrast, similar direct attribution is difficult to achieve in T-dominated basins. SHAP values derived from all flood events in T-dominated basins indicate that rainfall is also the most significant meteorological contributor to flashiness (Fig. 8b). However, the 95th percentile of rainfall during the study period has significantly decreased on average across all T-dominated basins (Fig. 8d), which would typically lead to a reduction in flashiness. Therefore, it is unlikely that rainfall is responsible for the observed increase in flashiness in these basins. Temperature shows a weak positive effect on flashiness, while soil moisture and snowmelt exhibit nonlinear or weak contributions (see Fig. S10 in Supporting Information S1). These results suggest that, among the hydrometeorological variables considered here, no single variable provides a robust explanation for the shortening of flood onset time in T-dominated basins. Therefore, the T-dominated response is more likely to reflect a complex combination of hydrological routing, antecedent catchment conditions, land-surface characteristics, and potentially unrepresented factors such as land-use change or soil hydraulic properties, rather than a direct climate-driven response (El Alfy, 2016).

## 5. Discussion

Event-based flashiness and river reach-based (or basin-based) flashiness capture distinct aspects of flash flood dynamics, each conveying unique physical meanings. Event-based flashiness measures the rate at which specific flood events intensify, with higher values indicating faster increases in flood volume per unit time, thus posing greater risks to human safety. In contrast, river reach-based (basin-based) flashiness reflects the risk of flash flooding in a specific river reach (basin). A higher level of river reach-based (basin-based) flashiness indicates a greater likelihood of flash flooding occurring in that area. Therefore, reaches with greater observed flashiness have a higher occurrence of flash floods (Fig. 2a, Fig. S11 in Supporting Information S1). Although there are no global-scale analyses of changes in flash flood risk, regional studies have observed the potential for greater flash flood risk in both occurrence and severity. Dougherty and Rasmussen (2020) found that flash flood–producing storms in the United States will not only increase runoff efficiency in a future climate but also be accompanied by higher rainfall intensity, which could exacerbate flash flood risks. Correspondingly, Ali et al. (2016) used a continental convective-permitting numerical weather model to project that U.S. floods will become flashier by the end of the century. Intense rainfall, as one of the main causes of flash floods, is also observed to have a tendency to be more intense and shorter in duration in North America and Europe (Wasko et al., 2021). This suggests a potentially heightened risk of flash floods in these regions, which aligns with the flashier flood hotspot areas identified in Fig. 2b.

Although GRFR has been validated against gauges, we acknowledge that discharge biases can be larger in cold and arid regions. To evaluate whether such uncertainty could affect the classification of cold/arid hotspots, we performed an additional Monte Carlo sensitivity test (Saltelli et al., 2008) using hourly USGS gauge validation results. Specifically, we used the bias in annual maximum discharge as a proxy for GRFR peak-discharge uncertainty and propagated this bias to GRFR-derived event flashiness. The analysis focused on cold/arid basins with significant increases in flashiness. Under 500 validation-based perturbations, the overall hotspot retention rate was 97.1%. The median probability of retaining the same Q/T-dominated class was 0.82, compared with a median class-change probability of 0.18 (see Fig. S12 in Supporting Information S1). These results suggest that validation-derived GRFR peak-discharge uncertainty does not substantially alter the main cold/arid hotspot conclusions, although a small number of basins show higher sensitivity.

To assess whether spatial dependence influenced the machine-learning attribution, we conducted an additional basin-blocked cross-validation (see Fig. S13 in Supporting Information S1). In this experiment, all event records from river reaches within the same basin were assigned to the same fold, ensuring that no basin was shared between the training and validation sets. The spatially blocked LightGBM model achieved an out-of-fold $R^2$ of 0.49 and a Pearson correlation coefficient of 0.70. As expected, this performance was lower than that obtained from random cross-validation, because basin-blocked validation provides a more stringent test of spatial transferability and because river basins differ substantially in their geographic, hydroclimatic, and

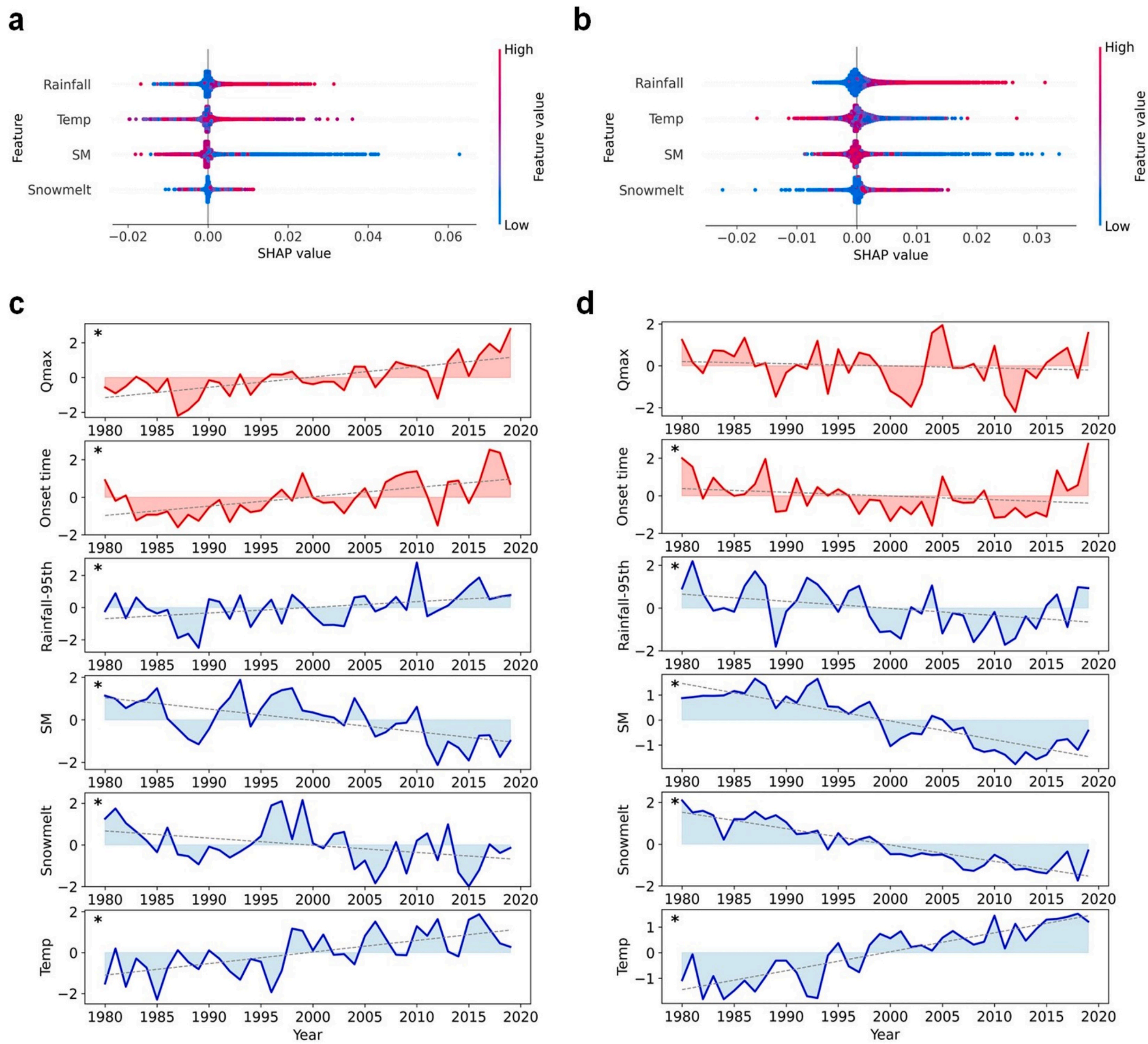


**Fig. 8.** Attribution of flashier floods in Q-dominated and T-dominated basins. Two basin types are presented: 51 basins with significantly ($p < 0.05$) increasing flash flood magnitude (left) and 28 basins with significantly decreasing onset time (right). (a and b) Feature importance of Q-dominated basins (a) and T-dominated basins (b) based on SHapley Additive exPlanations (SHAP) values from the LightGBM model, with the target variable being flood event flashiness. (c-d) Interannual variations of flood characteristics and associated variables over all Q-dominated basins (c) and T-dominated basins (d) from 1980 to 2019. The y-axis represents standardised anomalies. The grey dotted line indicates linear regression, and asterisks (*) denote statistically significant trends ($p < 0.05$), with p-values computed using the Mann-Kendall test.

geomorphological characteristics. Importantly, however, the resulting SHAP patterns remained broadly consistent with those from the main attribution analysis. This consistency indicates that the inferred hydroclimatic controls on flood flashiness are robust to spatially blocked validation and are unlikely to be primarily driven by local spatial leakage.

We also compared LightGBM with XGBoost and ultimately selected LightGBM based on model performance (Fig. 7, Fig. S14 in Supporting Information S1), with the target variable being flood event flashiness. We also conducted a SHAP analysis using the XGBoost model (see Fig. S15 in Supporting Information S1). While there are minor discrepancies compared to the SHAP results from the LightGBM model, likely due to variations in model structure and accuracy, the results are consistent overall. Both models demonstrate a positive contribution from high rainfall levels and low soil moisture. When soil moisture is low, a unit increase in soil moisture results in a substantial positive impact on flashiness. However, as soil moisture increases, the contribution of a unit change in soil moisture to flashiness diminishes, which aligns with Darcy's Law, suggesting that as soil water content rises, the soil infiltration rate converges to the permeability of saturated soil (Gavin & Xue, 2008). The effect of rainfall on flashiness is inverse; a unit change in rainfall contributes more significantly to flashiness when rainfall levels are high. Furthermore, neither temperature nor snowmelt exhibited a significant positive or negative effect. These findings lead to the same attribution result: the increase in flashiness in Q-dominated regions is primarily associated with the intensification of extreme rainfall. Nevertheless, this attribution should be interpreted with caution because the meteorological predictors are derived from gridded forcing products, including ERA5 and MSWEP, which inevitably contain uncertainties. Such uncertainties may affect the estimated contributions of rainfall, temperature, soil moisture, and snowmelt in the LightGBM and SHAP analyses, although they do not directly alter the GRFR-derived hotspot detection.

T-dominated basins do not have a single meteorological driver. This may be due to a complex combination of multiple factors or other influences (Gannon et al., 2022), such as changes in land surface characteristics. For example, Hirmas et al. (2018) found that under climate change, effective porosity might decrease in certain regions of the United States due to increases in mean annual precipitation and event magnitude, as well as decreases in atmospheric dryness and the frequency of freezing temperatures, leading to a significant reduction in saturated soil hydraulic conductivity. This reduction in conductivity suggests decreased infiltration, increased surface runoff, and greater susceptibility to flash floods. Vegetation coverage may also influence runoff generation during intense rainfall events (Ma et al., 2019), and changes in vegetation cover may trigger variations in flashiness. For Q-T compound basins, which are more complex in genesis, the causes may combine multiple factors from both T-dominated and Q-dominated basins, making analyses more difficult. We also acknowledge that changes in flood flashiness may be influenced by non-climatic factors. Changes in river-channel structure, such as channel incision or erosion, can increase flow celerity, thereby shortening flood response times (Sholtes & Doyle, 2011). In addition, land-surface changes such as urban expansion and deforestation can alter infiltration capacity, surface runoff generation, and runoff concentration (Ma et al., 2024; Miller et al., 2014), potentially modifying flood peaks and onset times. These unrepresented geomorphic and land-cover changes may introduce uncertainties in our interpretation of climate-zone patterns, particularly in rapidly urbanising or heavily modified basins. Exploring the possible mechanisms of flash floods would be challenging but a promising direction for unravelling the mystery of flash flood onset.

These contrasting forms of increasing flashiness also have implications for flood-risk management. In Q-dominated regions, larger floods may occur over similar durations, highlighting the need for flood defence infrastructure capable of withstanding more severe flood events. By comparison, in regions where shortened onset time is dominant, the intensity of floods may not change significantly, but floods are occurring over a shorter duration, reducing the available response time and increasing the challenges for early warning systems. This distinction has direct implications for risk management. In Q-dominated basins, adaptation should prioritise the reassessment of design flood standards, upgrading or reinforcing flood-control infrastructure, and revising floodplain management to account for larger peak discharges. In contrast, T-dominated basins require investments in rapid-response forecasting systems, higher-frequency hydrometeorological monitoring, nowcasting capacity, and emergency communication protocols, because the main challenge is the reduced lead time rather than necessarily larger flood magnitudes. Although relatively few, Q-T compound regions warrant particular attention due to their heightened dual vulnerability to both shorter warning times and more severe floods, making them especially susceptible to compounding risks.

The shift to flashier floods poses substantial challenges for flash flood monitoring and prediction (Younis et al., 2008). Many flash flood warning systems rely primarily on extreme rainfall thresholds (Georgakakos et al., 2022; Shamir et al., 2013), but watershed characteristics such as soil moisture, groundwater storage, vegetation cover, and land-use change can modify how rapidly rainfall is converted into runoff. To improve predictive accuracy, integrating additional variables like soil moisture and groundwater (Berghuijs & Slater, 2023) into flash flood models is crucial. Moreover, the impact of floods is influenced not only by their physical hazards but also by human responses to such events (Aerts et al., 2018). Advancing the understanding of flash flood risks requires further research, particularly in quantifying environmental, social, and economic vulnerabilities to flash floods and their broader impacts (Koks et al., 2015).

## 6. Conclusion

This study provides a global assessment of changes in flood flashiness from 1980 to 2019 using event-based flood information from GFRF. We find that nearly one-third of global basins have shifted towards flashier floods, with hotspots mainly located in North America, northwestern Asia, Europe, and parts of Africa and South America. By separating increasing flashiness into Q-dominated and T-dominated types, we show that flashier floods may emerge through either larger flood peaks or shorter onset times, implying different challenges for flood adaptation.

In Q-dominated basins, increasing extreme rainfall is the dominant meteorological factor associated with increasing flashiness among the variables considered. In contrast, T-dominated basins do not show a single robust hydrometeorological explanation, suggesting that shorter flood onset times may reflect more complex interactions among hydrological routing, antecedent catchment conditions, land-surface characteristics, and other unrepresented factors. These findings highlight the need for region-specific flood risk management strategies, including infrastructure designed for larger flood peaks and early warning systems adapted to shorter response times.

## Author contributions

F.Z. and S.W. conceived and designed the study. F.Z. carried out the calculations and analysis and then drafted the manuscript. S.T. assisted in the computation of the interpretable machine learning component. S. W. supported and supervised the study. Then, S.W., L.S., P.L., H.Y. and A.A. contributed to the improvement and modification of the draft. F.Z. revised and edited the manuscript.

## CRediT authorship contribution statement

**Fengjia Zhou:** Writing – original draft, Visualization, Validation, Methodology, Formal analysis, Data curation. **Shuo Wang:** Writing – review & editing, Supervision, Resources, Project administration, Investigation, Funding acquisition, Conceptualization. **Louise Slater:** Writing – review & editing. **Peirong Lin:** Writing – review & editing. **Hanbo Yang:** Writing – review & editing. **Sijie Tang:** Writing – review & editing. **Amir AghaKouchak:** Writing – review & editing.

## Declaration of competing interest

The authors declare that they have no known competing financial interests or personal relationships that could have appeared to influence the work reported in this paper.

## Acknowledgements

The work described in this paper was partially supported by a grant from the Research Grants Council of the Hong Kong Special Administrative Region, China (Project No. PolyU/RGC 15235324). LJS is supported by UKRI (MR/V022008/1) and NERC (NE/S015728/1).

## Appendix A. Supplementary data

Supplementary data to this article can be found online at https://doi.org/10.1016/j.jhydrol.2026.136163.

## Data availability

The GRFR 3-hourly flood data are available from Yang et al. (2021), and the underlying hydrography data are available at MERIT-Basins (Lin et al., 2019). The hourly datasets of precipitation, soil moisture, 2 m temperature, and snowmelt can be accessed from the ERA5 reanalysis (Hersbach et al., 2020). The hourly streamflow data in CONUS are available from USGS (http://waterdata.usgs.gov).

## References

Aerts, J.C.J.H., Botzen, W.J., Clarke, K.C., Cutter, S.L., Hall, J.W., Merz, B., Michel-Kerjan, E., Mysiak, J., Surminski, S., Kunreuther, H., 2018. Integrating human behaviour dynamics into flood disaster risk assessment. Nat. Clim. Chang. 8 (3), 193–199. https://doi.org/10.1038/s41558-018-0085-1.

Ahmadalipour, A., Moradkhani, H., 2019. A data-driven analysis of flash flood hazard, fatalities, and damages over the CONUS during 1996–2017. J. Hydrol. 578, 124106. https://doi.org/10.1016/j.jhydrol.2019.124106.
Ali, K., Bajracharya, R.M., Koirala, H.L., 2016. A review of flood risk assessment. Int. J. Environ. Agric. Biotechnol. 1 (4), 238636. https://doi.org/10.22161/ijeab/1.4.62.
Alipour, A., Ahmadalipour, A., Abbaszadeh, P., Moradkhani, H., 2020a. Leveraging machine learning for predicting flash flood damage in the Southeast US. Environ. Res. Lett. 15 (2), 024011. https://doi.org/10.1088/1748-9326/ab6edd.
Alipour, A., Ahmadalipour, A., Moradkhani, H., 2020b. Assessing flash flood hazard and damages in the southeast United States. J. Flood Risk Manage. 13 (2), e12605. https://doi.org/10.1111/jfr3.12605.
Baker, D.B., Richards, R.P., Loftus, T.T., Kramer, J.W., 2004. A new flashiness index: characteristics and applications to midwestern rivers and streams. JAWRA J. Am. Water Resour. Assoc. 40 (2), 503–522. https://doi.org/10.1111/j.1752-1688.2004.tb01046.x.
Barredo, J.I., 2007. Major flood disasters in Europe: 1950–2005. Nat. Hazards 42, 125–148. https://doi.org/10.1007/s11069-006-9065-2.
Beck, C., Grieser, J., Kottek, M., Rubel, F., Rudolf, B., 2006. Characterizing global climate change by means of Köppen climate classification. *Klimastatusbericht 2005*, 139–149 (2005).
Beck, H. E., Van Dijk, A. I., Levizzani, V., Schellekens, J., Miralles, D. G., Martens, B., De Roo, A., 2017. MSWEP: 3-hourly 0.25 global gridded precipitation (1979–2015) by merging gauge, satellite, and reanalysis data. *Hydrol. Earth Syst. Sci. 21*(1), 589–615. https://doi.org/10.5194/hess-21-589-2017.
Beck, H.E., Pan, M., Roy, T., Weedon, G.P., Pappenberger, F., Van Dijk, A.I., Huffman, G. J., Adler, R.F., Wood, E.F., 2019. Daily evaluation of 26 precipitation datasets using Stage-IV gauge-radar data for the CONUS. Hydrol. Earth Syst. Sci. 23 (1), 207–224. https://doi.org/10.5194/hess-23-207-2019.
Benfield, A., 2016. 2016 annual global climate and catastrophe report. [Available at http://thoughtleadership.aonbenfield.com/Documents/20140113_ab_if_annual_climate_catastrophe_report.pdf.].
Benjamini, Y., Hochberg, Y., 1995. Controlling the false discovery rate: a practical and powerful approach to multiple testing. J. Roy. Stat. Soc.: Ser. B (Methodol.) 57 (1), 289–300. https://doi.org/10.1111/j.2517-6161.1995.tb02031.x.
Berghuijs, W.R., Slater, L.J., 2023. Groundwater shapes north American river floods. Environ. Res. Lett. 18 (3), 034043. https://doi.org/10.1088/1748-9326/acbecc.
Bhaskar, N.R., French, M.N., Kyiamah, G.K., 2000. Characterization of flash floods in Eastern Kentucky. J. Hydrol. Eng. 5 (3), 327–331. https://doi.org/10.1061/(ASCE)1084-0699(2000)5:3(327).
Blöschl, G., Kiss, A., Viglione, A., Barriendos, M., Böhm, O., Brázdil, R., Coeur, D., Demarée, G., Llasat, M.C., Macdonald, N., 2020. Current European flood-rich period exceptional compared with past 500 years. Nature 583 (7817), 560–566. https://doi.org/10.1038/s41586-020-2478-3.
Chen, L., Yan, Z., Li, Q., Xu, Y., 2022. Flash flood risk assessment and driving factors: a case study of the Yantanxi River Basin, Southeastern China. Int. J. Disaster Risk Sci. 13 (2), 291–304. https://doi.org/10.1007/s13753-022-00408-3.
Donat, M.G., Lowry, A.L., Alexander, L.V., O'Gorman, P.A., Maher, N., 2016. More extreme precipitation in the world's dry and wet regions. Nat. Clim. Chang. 6 (5), 508–513. https://doi.org/10.1038/NCLIMATE2941.
Dottori, F., Szewczyk, W., Ciscar, J.-C., Zhao, F., Alfieri, L., Hirabayashi, Y., Bianchi, A., Mongelli, I., Frieler, K., Betts, R.A., 2018. Increased human and economic losses from river flooding with anthropogenic warming. Nat. Clim. Chang. 8 (9), 781–786. https://doi.org/10.1038/s41558-018-0257-z.
Dougherty, E., Rasmussen, K.L., 2020. Changes in future flash flood–producing storms in the United States. J. Hydrometeorol. 21 (10), 2221–2236. https://doi.org/10.1175/JHM-D-20-0014.1.
El Alfy, M., 2016. Assessing the impact of arid area urbanization on flash floods using GIS, remote sensing, and HEC-HMS rainfall–runoff modeling. Hydrol. Res. 47 (6), 1142–1160. https://doi.org/10.2166/nh.2016.133.
Fadhel, S., Rico-Ramirez, M.A., Han, D., 2018. Sensitivity of peak flow to the change of rainfall temporal pattern due to warmer climate. J. Hydrol. 560, 546–559. https://doi.org/10.1016/j.jhydrol.2018.03.041.
Feng, D., Gleason, C.J., 2024. More flow upstream and less flow downstream: the changing form and function of global rivers. Science 386 (6727), 1305–1311. https://doi.org/10.1126/science.adl5728.
Fowler, H.J., Lenderink, G., Prein, A.F., Westra, S., Allan, R.P., Ban, N., Barbero, R., Berg, P., Blenkinsop, S., Do, H.X., Guerreiro, S., Haerter, J.O., Kendon, E.J., Lewis, E., Schaer, C., Sharma, A., Villarini, G., Wasko, C., Zhang, X., 2021. Anthropogenic intensification of short-duration rainfall extremes. Nat. Rev. Earth Environ. 2 (2), 107–122. https://doi.org/10.1038/s43017-020-00128-6.
Gannon, J., Kelleher, C., Zimmer, M., 2022. Controls on watershed flashiness across the continental US. J. Hydrol. 609, 127713. https://doi.org/10.1016/j.jhydrol.2022.127713.
Gavin, K., Xue, J., 2008. A simple method to analyze infiltration into unsaturated soil slopes. Comput. Geotech. 35 (2), 223–230. https://doi.org/10.1016/j.compgeo.2007.04.002.
Georgakakos, K.P., Modrick, T.M., Shamir, E., Campbell, R., Cheng, Z., Jubach, R., Sperfslage, J.A., Spencer, C.R., Banks, R., 2022. The flash flood guidance system implementation worldwide: a successful multidecadal research-to-operations effort. Bull. Am. Meteorol. Soc. 103 (3), E665–E679. https://doi.org/10.1175/BAMS-D-20-0241.1.
Goodrich, K.A., Basolo, V., Feldman, D.L., Matthew, R.A., Schubert, J.E., Luke, A., Eguiarte, A., Boudreau, D., Serrano, K., Reyes, A.S., 2020. Addressing pluvial flash flooding through community-based collaborative research in Tijuana, Mexico. Water 12 (5), 1257. https://doi.org/10.3390/w12051257.
Gourley, J.J., Hong, Y., Flamig, Z.L., Arthur, A., Clark, R., Calianno, M., Ruin, I., Ortel, T., Wieczorek, M.E., Kirstetter, P.-E., 2013. A unified flash flood database across the United States. Bull. Am. Meteorol. Soc. 94 (6), 799–805. https://doi.org/10.1175/BAMS-D-12-00198.1.
Gourley, J.J., Flamig, Z.L., Vergara, H., Kirstetter, P.-E., Clark, R.A., Argyle, E., Arthur, A., Martinaitis, S., Terti, G., Erlingis, J.M., 2017. The FLASH project: improving the tools for flash flood monitoring and prediction across the United States. Bull. Am. Meteorol. Soc. 98 (2), 361–372. https://doi.org/10.1175/BAMS-D-15-00247.1.
Guerreiro, S.B., Fowler, H.J., Barbero, R., Westra, S., Lenderink, G., Blenkinsop, S., Lewis, E., Li, X.-F., 2018. Detection of continental-scale intensification of hourly rainfall extremes. Nat. Clim. Chang. 8 (9), 803–807. https://doi.org/10.1038/s41558-018-0245-3.
Hapuarachchi, H., Wang, Q., Pagano, T., 2011. A review of advances in flash flood forecasting. Hydrol. Process. 25 (18), 2771–2784. https://doi.org/10.1002/hyp.8040.
Hersbach, H., Bell, B., Berrisford, P., Hirahara, S., Horányi, A., Muñoz-Sabater, J., Nicolas, J., Peubey, C., Radu, R., Schepers, D., 2020. The ERA5 global reanalysis. Q. J. R. Meteorol. Soc. 146 (730), 1999–2049. https://doi.org/10.1002/qj.3803.
Hirabayashi, Y., Mahendran, R., Koirala, S., Konoshima, L., Yamazaki, D., Watanabe, S., Kim, H., Kanae, S., 2013. Global flood risk under climate change. Nat. Clim. Chang. 3 (9), 816–821. https://doi.org/10.1038/NCLIMATE1911.
Hirmas, D.R., Giménez, D., Nemes, A., Kerry, R., Brunsell, N.A., Wilson, C.J., 2018. Climate-induced changes in continental-scale soil macroporosity may intensify water cycle. Nature 561 (7721), 100–103. https://doi.org/10.1038/s41586-018-0463-x.
Jodar-Abellan, A., Valdes-Abellan, J., Pla, C., Gomariz-Castillo, F., 2019. Impact of land use changes on flash flood prediction using a sub-daily SWAT model in five Mediterranean ungauged watersheds (SE Spain). Sci. Total Environ. 657, 1578–1591. https://doi.org/10.1016/j.scitotenv.2018.12.034.
Jongman, B., Hochrainer-Stigler, S., Feyen, L., Aerts, J.C.J.H., Mechler, R., Botzen, W.J. W., Bouwer, L.M., Pflug, G., Rojas, R., Ward, P.J., 2014. Increasing stress on disaster-risk finance due to large floods. Nat. Clim. Chang. 4 (4), 264–268. https://doi.org/10.1038/nclimate2124.
Ke, G., Meng, Q., Finley, T., Wang, T., Chen, W., Ma, W., Ye, Q., Liu, T.-Y., 2017. Lightgbm: a highly efficient gradient boosting decision tree. Adv. Neural Inform. Process. Syst. 30.
Kemter, M., Merz, B., Marwan, N., Vorogushyn, S., Blöschl, G., 2020. Joint trends in flood magnitudes and spatial extents across Europe. Geophys. Res. Lett. 47 (7), e2020GL087464. https://doi.org/10.1029/2020GL087464.
Koks, E.E., Jongman, B., Husby, T.G., Botzen, W.J., 2015. Combining hazard, exposure and social vulnerability to provide lessons for flood risk management. Environ. Sci. Policy 47, 42–52. https://doi.org/10.1016/j.envsci.2014.10.013.
Konapala, G., Mishra, A.K., Wada, Y., Mann, M.E., 2020. Climate change will affect global water availability through compounding changes in seasonal precipitation and evaporation. Nat. Commun. 11 (1), 3044. https://doi.org/10.1038/s41467-020-16757-w.
Kvočka, D., Falconer, R.A., Bray, M., 2016. Flood hazard assessment for extreme flood events. Nat. Hazards 84 (3), 1569–1599. https://doi.org/10.1007/s11069-016-2501-z.
Lehner, B., Grill, G., 2013. Global river hydrography and network routing: baseline data and new approaches to study the world's large river systems. Hydrol. Process. 27 (15), 2171–2186. https://doi.org/10.1002/hyp.9740.
Li, Z., Gao, S., Chen, M., Gourley, J.J., Liu, C., Prein, A.F., Hong, Y., 2022. The conterminous United States are projected to become more prone to flash floods in a high-end emissions scenario. Commun. Earth Environ. 3 (1), 86. https://doi.org/10.1038/s43247-022-00409-6.
Li, Z., Gao, S., Chen, M., Zhang, J., Gourley, J.J., Wen, Y., Yang, T., Hong, Y., 2023. Introducing Flashiness-Intensity-Duration-Frequency (F-IDF): a new metric to quantify flash flood intensity. Geophys. Res. Lett. 50 (23), e2023GL104992. https://doi.org/10.1029/2023GL104992.
Lin, P., Pan, M., Beck, H.E., Yang, Y., Yamazaki, D., Frasson, R., David, C.H., Durand, M., Pavelsky, T.M., Allen, G.H., 2019. Global reconstruction of naturalized river flows at 2.94 million reaches. Water Resour. Res. 55 (8), 6499–6516. https://doi.org/10.1029/2019WR025287.
Looper, J.P., Vieux, B.E., 2012. An assessment of distributed flash flood forecasting accuracy using radar and rain gauge input for a physics-based distributed hydrologic model. J. Hydrol. 412, 114–132. https://doi.org/10.1016/j.jhydrol.2011.05.046.
Lundberg, S.M., Lee, S.I., 2017. A unified approach to interpreting model predictions. Adv. Neural Inf. Proces. Syst. 30.
Lundberg, S.M., Erion, G., Chen, H., DeGrave, A., Prutkin, J.M., Nair, B., Katz, R., Himmelfarb, J., Bansal, N., Lee, S.-I., 2020. From local explanations to global understanding with explainable AI for trees. Nat. Mach. Intell. 2 (1), 56–67.
Ma, M., Liu, C., Zhao, G., Xie, H., Jia, P., Wang, D., Wang, H., Hong, Y., 2019. Flash flood risk analysis based on machine learning techniques in the Yunnan Province. China. Rem. Sens. 11 (2), 170. https://doi.org/10.3390/rs11020170.
Ma, S., Zhou, S., Yu, B., Song, J., 2024. Deforestation-induced runoff changes dominated by forest-climate feedbacks. Sci. Adv. 10 (33), eadp3964. https://doi.org/10.1126/sciadv.adp3964.
Marchi, L., Borga, M., Preciso, E., Gaume, E., 2010. Characterisation of selected extreme flash floods in Europe and implications for flood risk management. J. Hydrol. 394 (1), 118–133. https://doi.org/10.1016/j.jhydrol.2010.07.017.
Meyer, J., Neuper, M., Mathias, L., Zehe, E., Pfister, L., 2021. More frequent flash flood events and extreme precipitation favouring atmospheric conditions in temperate regions of Europe. Hydrol. Earth Syst. Sci. Discuss. 2021, 1–28. https://doi.org/10.5194/hess-2021-628.

Miao, Q., Yang, D., Yang, H., Li, Z., 2016. Establishing a rainfall threshold for flash flood warnings in China's mountainous areas based on a distributed hydrological model. J. Hydrol. 541, 371–386. https://doi.org/10.1016/j.jhydrol.2016.04.054.

Miller, J.D., Kim, H., Kjeldsen, T.R., Packman, J., Grebby, S., Dearden, R., 2014. Assessing the impact of urbanization on storm runoff in a peri-urban catchment using historical change in impervious cover. J. Hydrol. 515, 59–70. https://doi.org/10.1016/j.jhydrol.2014.04.011.

Nguyen, P., Thorstensen, A., Sorooshian, S., Hsu, K., AghaKouchak, A., Sanders, B., Koren, V., Cui, Z., Smith, M., 2016. A high resolution coupled hydrologic–hydraulic model (HiResFlood-UCI) for flash flood modeling. J. Hydrol. 541, 401–420. https://doi.org/10.1016/j.jhydrol.2015.10.047.

Pedregosa, F., Varoquaux, G., Gramfort, A., Michel, V., Thirion, B., Grisel, O., Blondel, M., Prettenhofer, P., Weiss, R., Dubourg, V., 2011. Scikit-learn: machine learning in Python. J. Mach. Learn. Res. 12, 2825–2830.

Ragno, E., AghaKouchak, A., Love, C.A., Cheng, L., Vahedifard, F., Lima, C.H., 2018. Quantifying changes in future intensity-duration-frequency curves using multimodel ensemble simulations. Water Resour. Res. 54 (3), 1751–1764. https://doi.org/10.1002/2017WR021975.

Rentschler, J., Salhab, M., Jafino, B.A., 2022. Flood exposure and poverty in 188 countries. Nat. Commun. 13 (1), 3527. https://doi.org/10.1038/s41467-022-30727-4.

Saharia, M., Kirstetter, P.-E., Vergara, H., Gourley, J.J., Hong, Y., Giroud, M., 2017. Mapping flash flood severity in the United States. J. Hydrometeorol. 18 (2), 397–411. https://doi.org/10.1175/JHM-D-16-0082.1.

Saltelli, A., Ratto, M., Andres, T., Campolongo, F., Cariboni, J., Gatelli, D., Saisana, M., Tarantola, S., 2008. *Global Sensitivity Analysis: The Primer*. John Wiley & Sons.

Sene, K., 2012. *Flash Floods: Forecasting and Warning*. Springer Science & Business Media.

Shamir, E., Georgakakos, K.P., Spencer, C., Modrick, T., Murphy, M., Jubach, R., 2013. Evaluation of real-time flash flood forecasts for Haiti during the passage of Hurricane Tomas, November 4–6, 2010. Nat. Hazards 67, 459–482. https://doi.org/10.1007/s11069-013-0573-6.

Shapley, L.S., 1953. A value for n-person games. Contrib. Theory Games 2.

Sholtes, J.S., Doyle, M.W., 2011. Effect of channel restoration on flood wave attenuation. J. Hydraul. Eng. 137 (2), 196–208.

Sikorska, A.E., Viviroli, D., Seibert, J., 2015. Flood-type classification in mountainous catchments using crisp and fuzzy decision trees. Water Resour. Res. 51 (10), 7959–7976. https://doi.org/10.1002/2015WR017326.

Slater, L., Villarini, G., Archfield, S., Faulkner, D., Lamb, R., Khouakhi, A., Yin, J., 2021. Global changes in 20-year, 50-year, and 100-year river floods. Geophys. Res. Lett. 48 (6), e2020GL091824. https://doi.org/10.1029/2020GL091824.

Suardy, D. O., 2024. *Flash floods in Spain: joining forces for rapid recovery*. European Civil Protection and Humanitarian Aid Operations. Retrieved 2024-11-20 from https://civil-protection-humanitarian-aid.ec.europa.eu/news-stories/stories/.

Suriya, S., Mudgal, B.V., 2012. Impact of urbanization on flooding: the Thirusoolam sub watershed - a case study. J. Hydrol. 412–413, 210–219. https://doi.org/10.1016/j.jhydrol.2011.05.008.

Terti, G., Ruin, I., Anquetin, S., Gourley, J.J., 2017. A situation-based analysis of flash flood fatalities in the United States. Bull. Am. Meteorol. Soc. 98 (2), 333–345. https://doi.org/10.1175/BAMS-D-15-00276.1.

Ward, P.J., Jongman, B., Weiland, F.S., Bouwman, A., van Beek, R., Bierkens, M.F., Ligtvoet, W., Winsemius, H.C., 2013. Assessing flood risk at the global scale: model setup, results, and sensitivity. Environ. Res. Lett. 8 (4), 044019. https://doi.org/10.1088/1748-9326/8/4/044019.

Wasko, C., Nathan, R., Stein, L., O'Shea, D., 2021. Evidence of shorter more extreme rainfalls and increased flood variability under climate change. J. Hydrol. 603, 126994. https://doi.org/10.1016/j.jhydrol.2021.126994.

Yang, Y., Pan, M., Lin, P., Beck, H.E., Zeng, Z., Yamazaki, D., David, C.H., Lu, H., Yang, K., Hong, Y., 2021. Global reach-level 3-hourly river flood reanalysis (1980–2019). Bull. Am. Meteorol. Soc. 102 (11), E2086–E2105. https://doi.org/10.1175/BAMS-D-20-0057.1.

Yin, J., Gao, Y., Chen, R., Yu, D., Wilby, R., Wright, N., Ge, Y., Bricker, J., Gong, H., Guan, M., 2023. Flash floods: why are more of them devastating the world's driest regions? Nature 615, 212–215.

You, J., Wang, S., 2021. Higher probability of occurrence of hotter and shorter heat waves followed by heavy rainfall. Geophys. Res. Lett. 48 (17), e2021GL094831. https://doi.org/10.1029/2021GL094831.

You, J., Wang, S., Zhang, B., 2024. Spatially seamless and temporally continuous assessment on compound flood risk in Hong Kong. J. Hydrol. 645, 132217. https://doi.org/10.1016/j.jhydrol.2024.132217.

Younis, J., Anquetin, S., Thielen, J., 2008. The benefit of high-resolution operational weather forecasts for flash flood warning. Hydrol. Earth Syst. Sci. 12 (4), 1039–1051. https://doi.org/10.5194/hess-12-1039-2008.

Zhang, S., Zhou, L., Zhang, L., Yang, Y., Wei, Z., Zhou, S., Yang, D., Yang, X., Wu, X., Zhang, Y., 2022. Reconciling disagreement on global river flood changes in a warming climate. Nat. Clim. Chang. 12 (12), 1160–1167. https://doi.org/10.1038/s41558-022-01539-7.

Zhong, M., Jiang, T., Li, K., Lu, Q., Wang, J., Zhu, J., 2020. Multiple environmental factors analysis of flash flood risk in Upper Hanjiang River, southern China. Environ. Sci. Pollut. Res. 27, 37218–37228. https://doi.org/10.1007/s11356-019-07270-9.

Zhou, M., Wang, S., Peng, D., 2025. Economic losses from typhoon-induced coastal flooding in Hong Kong under future climate change. J. Hydrol. 661, 133569. https://doi.org/10.1016/j.jhydrol.2025.133569.

Zhu, P., Kim, T., Jin, Z., Lin, C., Wang, X., Ciais, P., Mueller, N.D., Aghakouchak, A., Huang, J., Mulla, D., 2022. The critical benefits of snowpack insulation and snowmelt for winter wheat productivity. Nat. Clim. Chang. 12 (5), 485–490. https://doi.org/10.1038/s41558-022-01327-3.